Title

Seismic Response Analysis of a Highway Overcrossing Equipped with Elastomeric Bearings and Fluid Dampers

Journal

Journal of Structural Engineering, 130(6)

Authors

Makris, Nicos
Zhang, Jian

Publication Date

2004

Peer reviewed

Seismic Response Analysis of a Highway Overcrossing Equipped with Elastomeric Bearings and Fluid Dampers

Nicos Makris, M.ASCE,[1] and Jian Zhang, A.M.ASCE[2]

Abstract: This paper presents a case study on the seismic response of a recently constructed freeway overcrossing located in southern California, which is equipped with elastomeric bearings and fluid dampers at its end abutments. The analysis employs the substructure method and a reduced order stick model. The macroscopic constitutive laws of the springs and dashpots that approximate the mechanical behavior of approach embankments, pile foundations, center bent, abutments, elastomeric bearings, and fluid dampers are established in the companion paper. The paper presents an in-depth analysis of the seismic response of the bridge equipped with the response modification devices accounting for the effects of soil–structure interaction. The various response quantities presented are compared with the corresponding response quantities of a hypothetical bridge with integral abutments. Advantages and challenges in the two design configurations are identified and discussed.

DOI: 10.1061/(ASCE)0733-9445(2004)130:6(830)

CE Database subject headings: Overpasses; Seismic response; Bearing capacity; Damping; Soil-structure interaction.

Introduction

Most conventionally designed bridges use elastomeric bearings (pads) between the deck and its supports to accommodate thermal movements. The long experience with this technology had a positive role on the implementation of modern seismic protection technologies in bridges. A number of bridges worldwide are now equipped with seismic protective bearings that engage some energy dissipation mechanism (Skinner et al. 1993). The most commonly used seismic isolation system consists of lead–rubber bearings that combine the function of isolation and energy dissipation in a single compact unit, while also supporting the weight of the superstructure and providing restoring force. Sliding bearings allow for appreciable mobility and provide energy dissipation through friction. In this case, an additional restoring mechanism is often added to provide the structure with some reentering capacity. Spherical sliding bearings provide the designed restoring mechanism because of their curvature, while at the same time dissipate energy.

The traditional nonseismic elastomeric pads used in bridges for thermal movements can provide some limited seismic protection, however their integrity during large displacements might be substantially deteriorated or even destroyed due to shearing of the elastomer or rolling of the entire bearing. Accordingly, elastomeric pads with improved seismic performance have been developed (ATC 1993; ATC 2002) while their displacement and stress demands are established in design specification documents (FHWA 1995; AASHTO 1999). The increasing need for safer bridges, in association with the rapid success of seismic protection devices in buildings, has accelerated the implementation of large-capacity damping devices in bridges. The Vincent Thomas suspended bridge in southern California (Smyth et al. 2000), the Rion-Antirion cable-stayed bridge in western Greece (Papanikolas 2002), and the 91/5 highway overcrossing in southern California are examples of bridges that have been equipped with fluid dampers.

The promises of modern seismic protection technologies about their ability to operate under strong shaking has directed most of the attention on the performance of bearings and dampers under large displacements and large velocities. The interaction of these devices with the remaining bridge structure is an issue that has been either incorporated in the response analysis indirectly via finite element analysis of the entire bridge with large computer codes or has been neglected; partly because the transmitting forces are usually relatively small and the reaction structures are usually relatively stiff.

In this paper, the efficiency of modern seismic protection technologies is examined by analyzing the seismic response of a newly constructed highway overcrossing in southern California. The 91/5 Overcrossing of interest is supported at each end abutment on four elastomeric pads while it is attached with four fluid dampers. The deck is supported monolithically near its center span by a prestressed reinforced concrete outrigger. The interesting characteristic of this structure is that its transverse and longitudinal modal periods lie in the range between 0.4 s and 0.8 s. That is a period range for which supplemental damping on a single-degree-of-freedom structure has a beneficial effect. Furthermore, the bridge is approached from each side by earth embankments that have a tendency to amplify the free-field motion and increase the role of soil–structure interaction. Accordingly, the assessment of the efficiency of the seismic protection devices is conducted by accounting for in our analysis the effect of soil–structure interaction at the end abutments/approach embankments and at the foundations of the center columns. In principle, length-

[1]Professor, Univ. of California, Berkeley, CA 94720.

[2]Assistant Professor, Univ. of Illinois at Urbana–Champaign, Urbana, IL 61801; formerly, Graduate Student Researcher, Univ. of California, Berkeley, CA 94720.

Note. Associate Editor: Andrei M. Reinhorn. Discussion open until November 1, 2004. Separate discussions must be submitted for individual papers. To extend the closing date by one month, a written request must be filed with the ASCE Managing Editor. The manuscript for this paper was submitted for review and possible publication on July 1, 2002; approved on August 7, 2003. This paper is part of the ***Journal of Structural Engineering***, Vol. 130, No. 6, June 1, 2004. ©ASCE, ISSN 0733-9445/2004/6-830–845/$18.00.

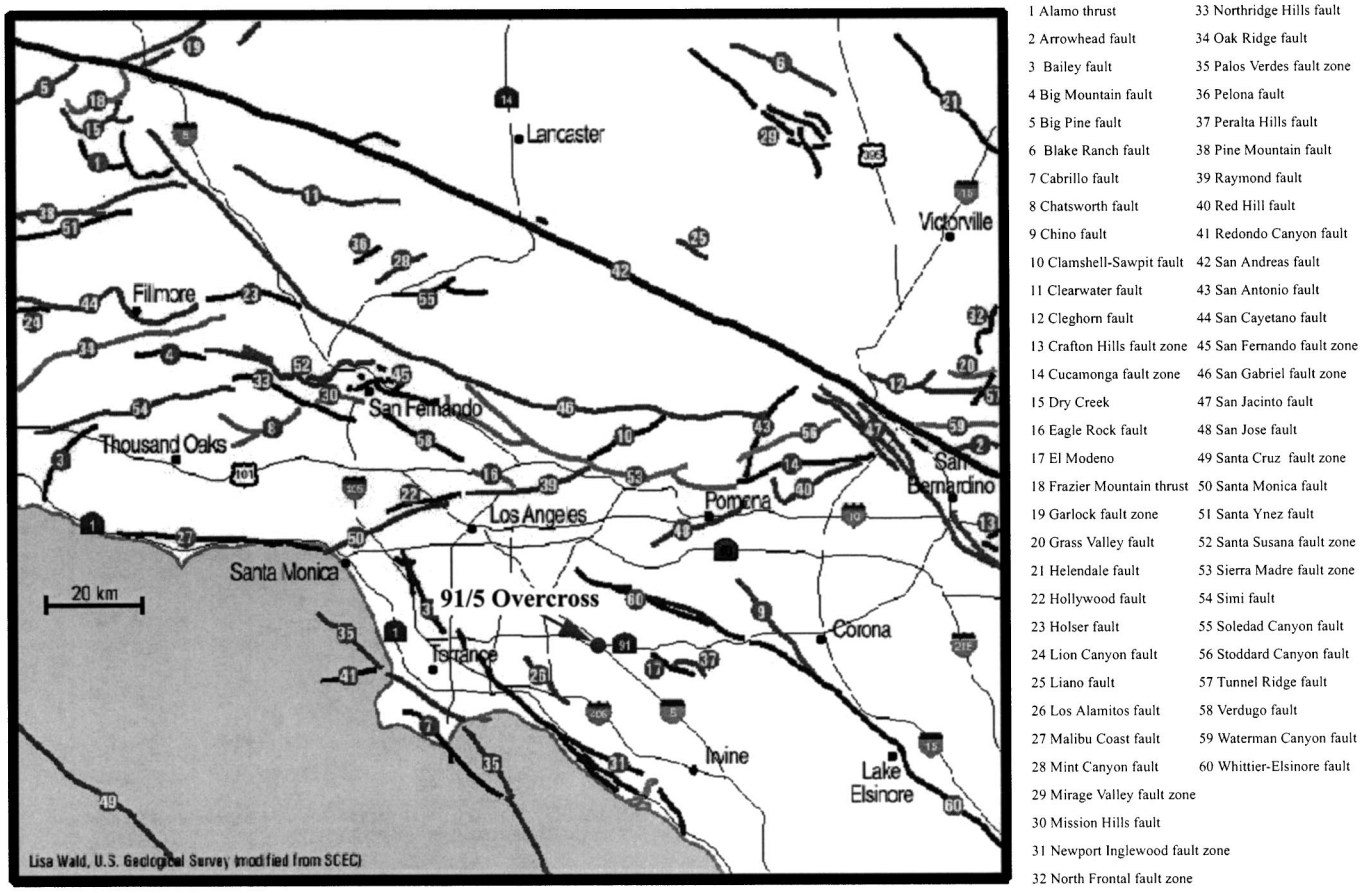

Fig. 1. Location of 91/5 Overcrossing and traces of nearby faults

ening the period of a structure with mechanical isolation reduces accelerations and increases displacements. Nevertheless, a more flexible configuration offers the deck additional mobility that may result in an undesirable response.

Location, Structural Configuration and Geotechnical Information

Location and Selection of Ground Motions

Fig. 1 shows the location of the 91/5 Overcrossing in the greater Los Angeles area together with the traces of the nearby faults. The Whittier–Elsinore fault is 11.6 km (7.2 miles) to the northeast, while the Newport Inglewood fault zone is 20 km (12.5 miles) to the southwest.

Because of the proximity of the bridge to active faults, the thrust of this analysis is placed to near-source ground motions that exhibit distinguishable strong acceleration and velocity pulses. The response of the bridge structure with various levels of damping when subjected to near-source and pulse-type motions has been investigated by Makris and Chang (1998, 2000a,b) and an experimental investigation with an emphasis on short bridges has been presented by Chang et al. (2002). These studies that concentrated on the seismic response of a rigid block supported on a variety of isolators concluded that for all ground motions examined an increase of viscous damping ratio from 14% to 50% reduce the base displacement by half or even more without appreciably increasing base accelerations.

In this study the structural system of interest is more complicated not only because of the flexibility of the deck, but also because of the effects of soil–structure interaction between the bridge and the approach embankment. In order to investigate this problem, we use eleven strong ground motions that have been recorded in California relatively close to the fault of major earthquakes. Table 1 lists in historic order the records of interest together with the magnitude of the earthquake and distance of the accelerograph from the causative fault. The time histories of these ground motions can be found in the papers by Makris and Chang (1998) and references reported therein.

Structural Configuration

The newly constructed 91/5 Overcrossing is a continuous two-span, cast-in-place, prestressed concrete, box-girder bridge supported by an outrigger bent at midspan and equipped with four fluid dampers at each end abutment (eight dampers total). The bridge has two spans of 192 ft (58.5 m) long spanning a four-lane highway. Its two abutments are skewed at 33°. The width of deck along the east span is about 42.5 ft. (12.95 m) while the width along the west span is about 49.2 ft (15 m). The cross section of the deck consists of three cells. The deck is supported by a 103 ft (31.4 m) long prestressed outrigger beam which rests on two pile groups, each consisting of 49 driven concrete friction piles. The columns are approximately 22.5 ft (6.9 m) high.

At each abutment, the deck rests on four elastomeric pads. Fig. 2 presents the elevation and plan views of the bridge. The total weight of the deck (including outrigger beam) is approximately

Table 1. Earthquake Records Selected for Simulation

Record station	Earthquake	Magnitude (M_w)	Distance to fault (km)	Peak acceleration (g)[a]	Peak velocity (m/s)
Pacoima Dam	1971 San Fernando	6.6	8.5	1.17 (1.08)	1.14 (0.57)
El Centro Array No. 5	1979 Imperial Valley	6.4	30.4	0.38 (0.53)	0.99 (0.52)
El Centro Array No. 6	1979 Imperial Valley	6.4	29.8	0.44 (0.34)	1.13 (0.68)
El Centro Array No. 7	1979 Imperial Valley	6.4	29.4	0.46 (0.34)	1.13 (0.55)
Parachute test site	1987 Superstition Hills	6.6	7.2	0.45 (0.38)	1.12 (0.44)
Los Gatos	1989 Loma Prieta	7.0	6.1	0.56 (0.61)	0.95 (0.51)
Cape Mendocino	1992 Petrolia	7.0	3.8	1.50 (1.04)	1.25 (0.41)
Lucerne Valley	1992 Landers	7.3	42.0	0.71 (0.80)	1.36 (0.70)
Rinaldi	1994 Northridge	6.7	9.9	0.89 (0.39)	1.75 (0.60)
Sylmar	1994 Northridge	6.7	12.3	0.73 (0.60)	1.22 (0.54)
Newhall	1994 Northridge	6.7	20.2	0.59 (0.58)	0.96 (0.75)

[a]Peak acceleration values are for the fault normal component. The values of the fault parallel component are offered in parentheses.

25 MN, whereas the weight of each abutment is approximately 5 MN. The distribution of vertical reactions is also shown in Fig. 2 below the elevation. Since each abutment supports approximately 4 MN, each pad carries a vertical load of approximately 4 MN/4 = 1 MN. The bridge is equipped with eight hydraulic dampers, four at the each end, connecting the deck with the abutments as shown in Fig. 3. With this arrangement, the dampers engaged in both longitudinal and transverse motions of the deck. A photograph of the four fluid dampers installed at the east abutment is shown in Fig. 1 of the companion paper. The cross section of the bridge along the outrigger and a plan view of the pile group is shown in Fig. 3 of the companion paper (Zhang et al. 2004).

Geotechnical Data

Before construction, a geotechnical exploration at the location of the piers and near the end abutments was conducted. Using standard penetration test (SPT) measurements from the ground surface down to a depth about 35 m, moderately stiff soil were identified, which consisted of silty and clayey sand, sandy silt to clayey silt, and occasionally gravelly sand and gravel. SPT blow counts varied from 8 to 70 blows/count. The averaged soil density is about $\rho = 1{,}800\ \text{kg/m}^3$. Fig. 4 summarizes the results of the geotechnical exploration along with the SPT blow counts for each soil layer. Empirical formulas have been proposed in literature in order to correlate the SPT blow counts and the maximum shear modulus of sand, $G_{\max}$. For example,

$$G_{\max} \approx 35 N_{60}^{0.68} \ (\text{kips/ft}^2) \quad \text{(Imai and Tonouchi 1982)} \quad (1)$$

or

$$G_{\max} = 35 N_{60}^{0.34} (\overline{\sigma}_v)^{0.4} \ (\text{kips/ft}^2) \quad \text{(Seed et al. 1986)} \quad (2)$$

where N_{60} = blow count number measured in SPT test delivering 60% of the theoretical free-fall energy to the drill rod; and $\overline{\sigma}_v$ = effective vertical stress (lb/ft^2). These two empirical relationships are widely used within a number of publications that correlate results. The inherent difficulty of correlating a small strain parameter $G_{\max}$ with a penetration test that relates to much larger

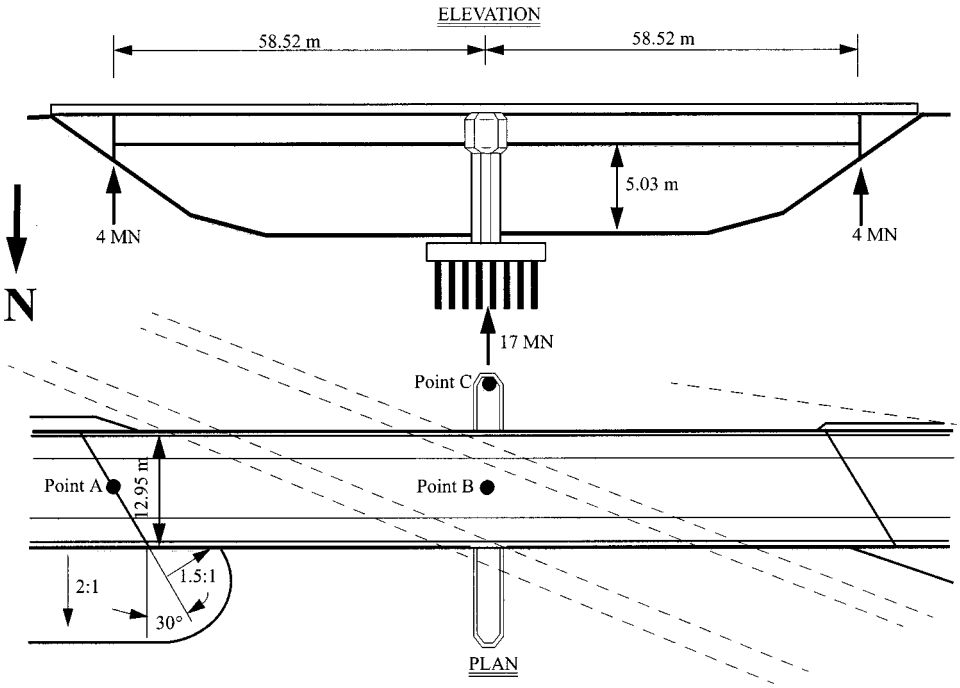

Fig. 2. Elevation and plan views of 91/5 Overcrossing

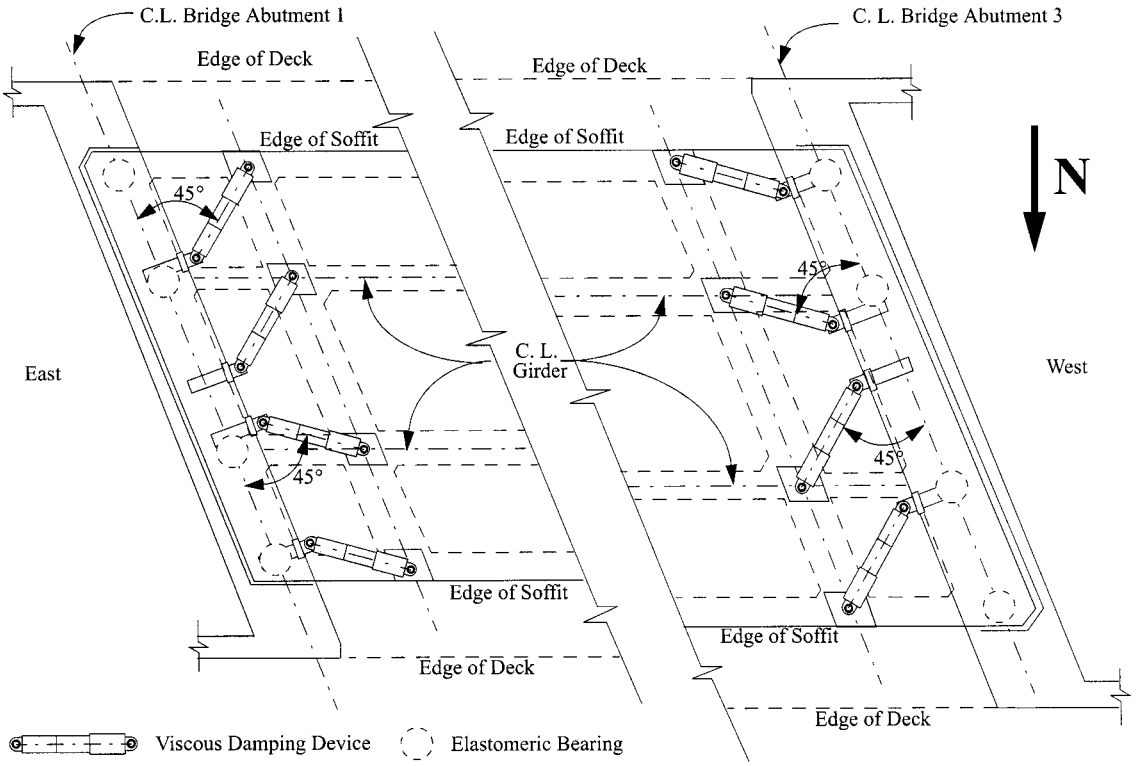

Fig. 3. Layout of eight fluid dampers installed at end abutments and locations of elastomeric pads

strains is evident from the scatter in the data on which they are based and from the variability of the results obtained by different investigators (Kramer 1996). Therefore, Eqs. (1) and (2) are only used to give a preliminary estimate of G_{max}. The small strain shear modulus G_{max} varies from 64 MPa to 240 MPa. These values were derived from SPT blow counts in the range of 8 and 30 according to Eq. (1), whereas Eq. (2) indicates that the shear modulus G_{max} is an increasing function with depth. At depth 20 ft, an average blow count 30 results in G_{max} of 84 MPa. Given the variability of data, the value of G_{max}=72 MPa is adopted in this study which results in a shear wave velocity of 200 m/s. Poisson's ratio of soil is assumed to be 0.4.

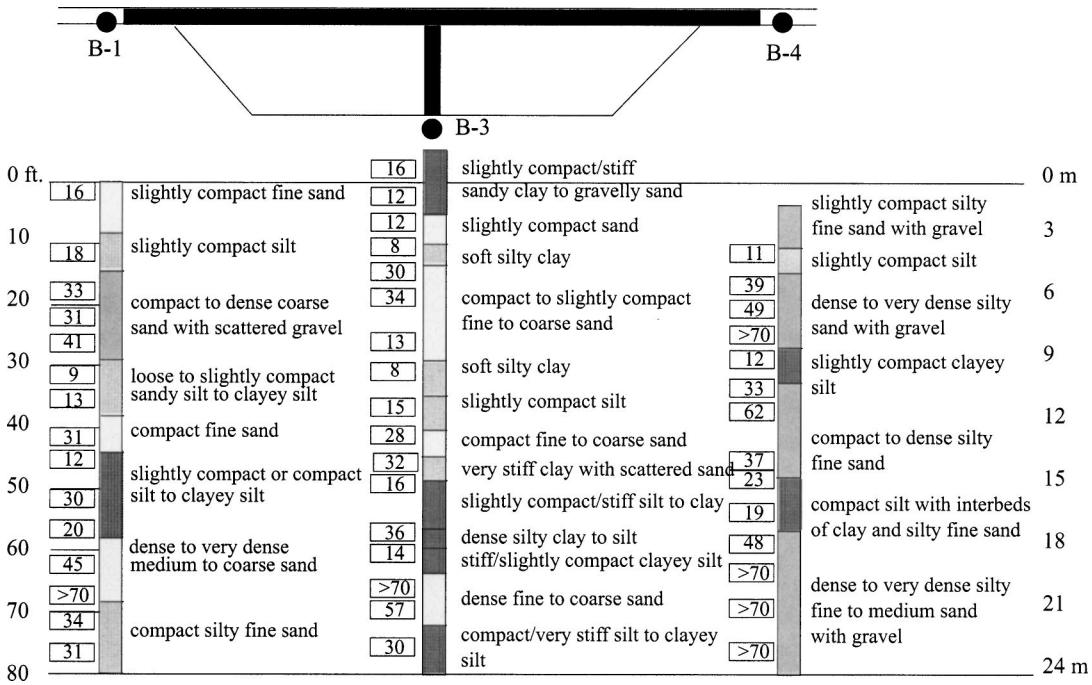

Fig. 4. Three soil profiles of 91/5 Overcrossing site (numerical values in boxes are blow counts by standard penetration test)

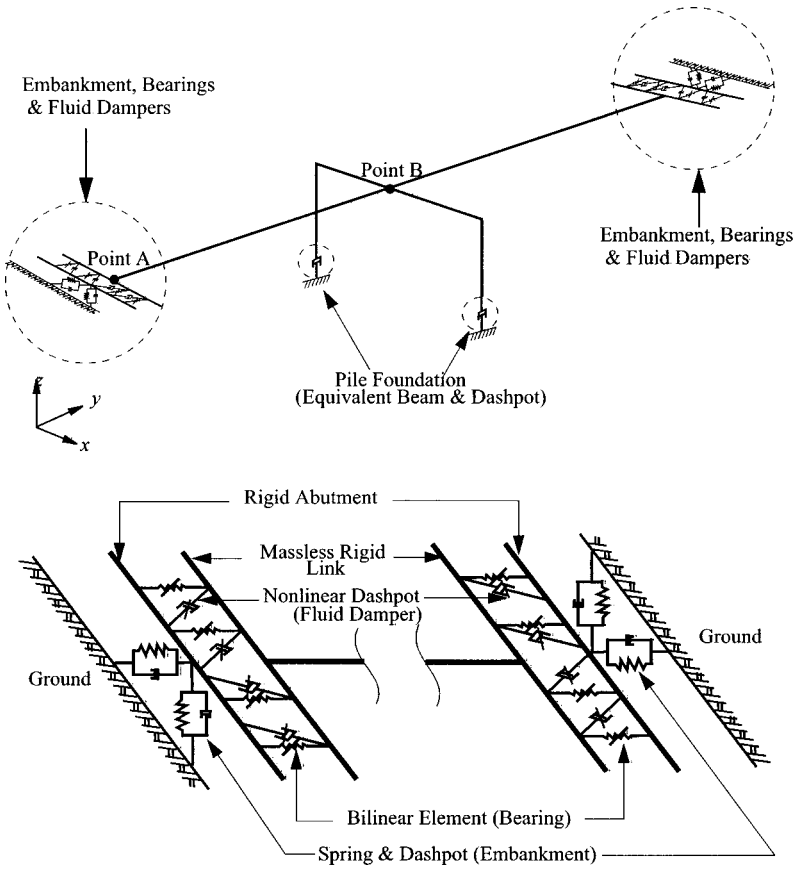

Fig. 5. Top: Structural idealization of the 91/5 Overcrossing with beam elements and frequency independent springs and dashpots; bottom: Detail of the mechanical model that transfer forces from the deck to the surrounding soil

Seismic Response Analysis

Fig. 5 (top) shows a stick model idealization of the 91/5 Overcrossing. The stick model was introduced by Maragakis and Jennings (1987) and its validity was investigated by McCallen and Romstad (1994). Additional studies that confirmed its validity have been conducted by Zhang and Makris (2001, 2002b).

The stick model is a collection of beam elements with cross section properties adjusted from geometric data without considering any cracked section reduction. At each end, a massless rigid link preserves the skewed geometry of the bridge and serves as the connecting element between the bridge deck and the end abutments. The spring and dashpot values of the approach embankments and pile foundations have been estimated with the methodologies summarized in the companion paper (Zhang et al. 2004). Additional information on the dynamic stiffness of approach embankments can be found in the references by Zhang and Makris (2001, 2002a); whereas, additional information on the dynamic stiffnesses of pile groups can be found in the paper by Makris et al. (1994) and references reported therein. All values of interest are summarized in Table 2. The behavior of the elastomeric pads is modeled with the two-dimensional plasticity model presented in the companion paper (Zhang et al. 2004); whereas the behavior of the nonlinear fluid damper is expressed with a nonlinear power law also presented in the companion paper with Eq. (32).

During the numerical simulation, Young's modulus of the beam elements on top of the column was artificially increased by three orders of magnitude to form a rigid link in order to prevent excessive deflections at the connection point between the center columns and the outrigger beam (McCallen and Romstad 1994). Vertical excitations are not considered. In both models, the damping of the bridge deck and center bent is approximated with the Rayleigh damping approximation, where the parameters α and β are computed by assuming a 5% modal damping ratio in the first and the second modes. Young's modulus of the concrete is assumed to be $E_c = 22$ GPa. This value is approximately 80% of the value obtained from empirical expressions to account for the cracking that occurred during the earthquake. Similar cracked values for Young's modulus of concrete in the seismic response analysis of bridges have been reported by Douglas and Reid [(1982), $E_c = 20-25$ GPa] and Dendrou et al. [(1985), $E_c = 20$ GPa]. The density of concrete is assumed 2,400 kg/m^3.

In this paper, we compare the dynamic response of three configurations of the 91/5 Overcrossing:

1. The as-built configuration where the deck is supported at both ends by elastomeric pads and is equipped with fluid dampers (pads and dampers),
2. Same configuration as case 1 but without fluid dampers (pads only), and
3. The bridge deck is rigidly connected to integral abutments (integral abutments).

For the analysis of all three cases, the same stick model shown in Fig. 5 is employed. For the analysis of Case 2, the dampers between the abutments and the massless rigid links are removed; whereas for the analysis of Case 3, the springs and dashpots between the abutments and the massless rigid links are locked.

Table 2. Spring and Dashpot Values that Approximate the Presence of the Approach Embankments and Pile Foundation of the 91/5 Overcrossing. Values under Case 1 Correspond to Strong Shaking whereas Values under Case 2 Correspond to Moderately Strong Shaking

Parameters	Case 1	Case 2
Embankment + pile foundations		
K_x (MN/m)	119 + 292 (119 + 271)	238 + 488 (238 + 453)
K_y (MN/m)	119 + 293 (119 + 272)	238 + 490 (238 + 456)
K_z (MN/m)	451 + 1,135 (451 + 1,058)	892 + 1,586 (892 + 1,478)
C_x (MN·s/m)	11 + 28 (11 + 24)	13 + 32 (13 + 28)
C_y (MN·s/m)	11 + 22 (11 + 17)	13 + 26 (13 + 19)
C_z (MN·s/m)	14 + 128 (14 + 101)	27 + 124 (27 + 98)
Pile foundation of center bent		
K_x, K_y (MN/m)	492	821
K_r (MN·m/rad)	31,739	44,187
K_{xr}, K_{yr} (MN/rad)	−811	−1,138
K_z (MN/m)	1,452	2,020
C_x, C_y (MN·s/m)	14.5	16.2
C_z (MN·s/m)	54.3	50.2

Note: Case 1: $G = 10$ MPa, $\eta = 0.5$ at abutment; $G = 28$ MPa, $\eta = 0.35$ at center bent. Case 2: $G = 20$ MPa, $\eta = 0.4$ at abutment; $G = 56$ MPa, $\eta = 0.12$ at center bent. Numbers in parentheses are the values of west abutment.

Eigenvalue Analysis

For the eigenvalue analysis, it is assumed that the deck displacements are small enough ($u_{\text{deck}} < u_y$) so the elastomeric pads deform within the preyielding range exhibiting, in each direction, a stiffness

$$K_x = K_y = 8K_1 = 40 \ \text{MN/m} \tag{3}$$

where K_1 is given by Eq. (28) of the companion paper (Zhang et al. 2004). The nonlinear fluid dampers are replaced with linear dashpots that dissipate the same amount of energy as dictated by Eq. (41) of the companion paper. The nominal amplitude of motion, u_0, appearing in that equation is associated with the level of excitation. At a displacement of $u_0 \approx 6$ cm (2.3 in.), the elastomeric pads still operate within the preyielding range exhibiting the stiffness value given by Eq. (3). Furthermore, time–history analysis under several moderately strong ground motions resulted in the damper displacement being $u_0 \approx 2.0$–2.3 in. Accordingly, the nominal amplitude $u_0 \approx 5$ cm (2 in.). The frequency, ω, appearing in Eq. (41) of the companion paper (Zhang et al. 2004), is equal to the first modal undamped frequency ($\omega = \omega_1$).

Eigensolutions are performed for the bridge with integral abutments and the bridge with protective devices (elastomeric pads and fluid dampers) using the commercially available software *ABAQUS* (1997). Since the fluid dampers do not provide any stiffness, the bridge with pads only (Case 2) essentially yields the same modes and modal frequencies as that of the bridge equipped with both pads and fluid dampers (Case 1). Fig. 6 depicts the first six mode shapes as well as the natural frequencies of the bridge equipped with integral abutments (left-hand side) and that of the bridge with pads and fluid dampers (right-hand side), where the soil properties are taken as $G = 20$ MPa and $\eta = 0.4$ at end abutments and $G = 56$ MPa and $\eta = 0.12$ at center bent (Case 2).

For the bridge with integral abutment, the first mode shape is antisymmetric vertical, while the second mode shape is symmetric vertical. The third is the first transverse mode that indicates lateral flexure of the deck. When the bridge is sitting on elastomeric pads at each end, the structural configuration is more flexible. Accordingly, the modal frequencies of the bridge sitting on elastomeric pads at each end are smaller than the modal frequencies of the bridge with integral abutments. As a result, the first mode is longitudinal, the second mode is torsional about the vertical axis while the third mode is antisymmetric vertical. The first transverse mode of the isolated configuration is the fourth mode that indicates more of a rigid body translation of the deck rather than flexure which is observed in the third mode of the bridge with integral abutment. Table 3 compares the first six natural frequencies of the bridge with integral abutment and the bridge with protective devices when soil properties are taken as: $G = 20$ MPa, $\eta = 0.40$ at abutment and $G = 56$ MPa, $\eta = 0.12$ at center bent (Case 2).

Modal damping ratios are estimated with the complex eigenvalue procedure presented in Zhang and Makris (2001, 2002b). A reduced-order stick model was developed with fewer degrees of freedom in order to bypass the problem of computing and interpreting the large number of complex eigenvalues resulting from the original stick model. For simplicity, the reduced-order stick model lumped the four fluid dampers into two orthogonal nonlinear dashpots rather than preserving the exact layout as shown in Fig. 5. Similarly, the presence of the embankment and elastomeric pads are represented by two orthogonal springs and dashpots respectively, as shown in Fig. 5.

Table 3 compares the first six modal frequencies and modal damping ratios of a bridge with integral abutment, a bridge with pads, and a bridge with pads and nonlinear fluid dampers under different levels of earthquakes. It is worth mentioning that the natural modes of a bridge with integral abutments are different from that of the bridge with elastomeric pads and/or nonlinear fluid dampers. Therefore, a one-to-one comparison of modal damping ratios between these two cases is not meaningful. A more meaningful comparison is between the case with pads only and the case with pads and dampers. Some key observations from Table 3 are:

- The behavior of the bridge configuration with integral abutments is essentially very similar to that of the Meloland Road Overcrossing and the Painter Street Bridge (Zhang and Makris 2001; 2002b), where high modal damping ratios are associated with the longitudinal and transverse modes that mobilize a large volume of soil with high damping.
- The first transverse mode of the bridge with integral abutment

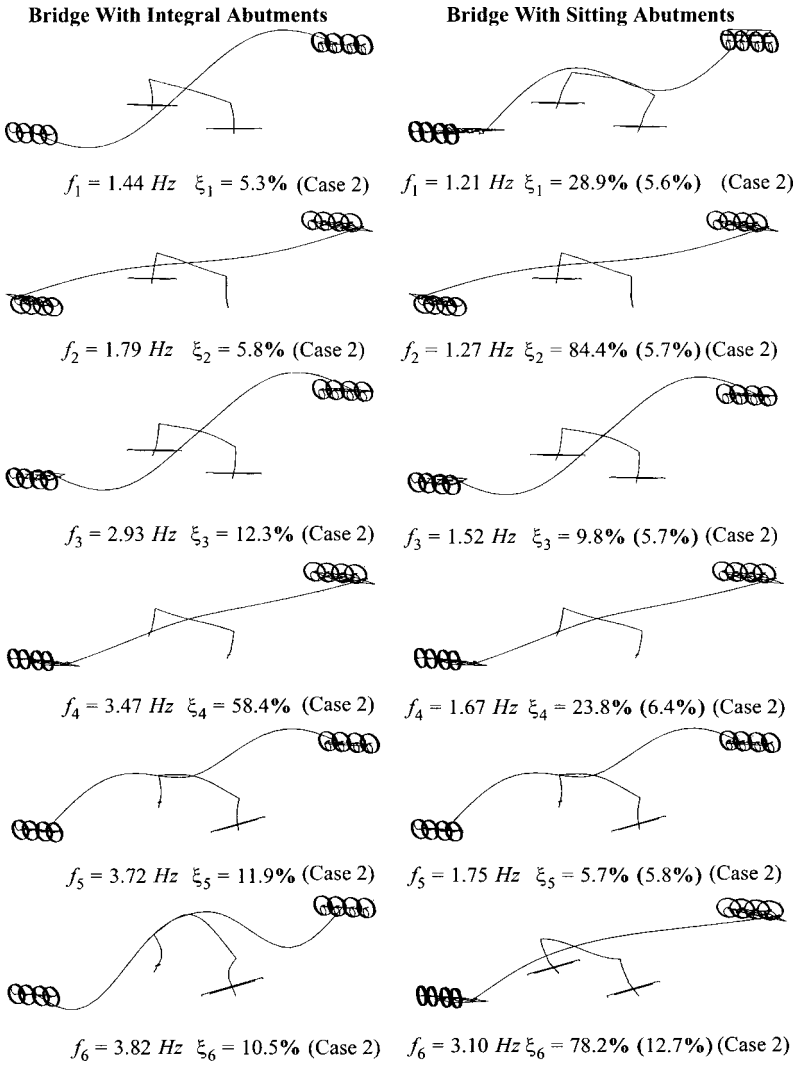

Fig. 6. First six modal frequencies, damping ratios, and mode shapes computed with stick model of 91/5 Overcrossing (left-hand side: Bridge with integral abutments; right-hand side: Bridge with sitting abutments). The damping ratios in parentheses are for the bridge with pads only

(Case 3) is a flexural mode, whereas the first transverse mode of the bridge with pads (Cases 1 and 2) is essentially a translational mode.

- Because of the flexibility introduced by elastomeric pads at the deck ends, the modal damping ratios associated with the longitudinal or transverse modes of the isolated bridge are appreciably smaller than the modal damping ratios of the bridge with integral abutment since the bridge superstructure can move substantially without mobilizing large volumes of soil. At the same time, the modal frequencies of the bridge with pads are lower than that of the bridge with integral abutments.
- When integral abutments are considered, the modal damping along the longitudinal direction is 58% and along the transverse direction is 12%. When pads and dampers are added, the situation reverses. Because of the flexibility of the pads, the bridge moves appreciably both in the longitudinal and transverse directions. Along the longitudinal direction, the modal damping of the bridge with pads and dampers is approximately 28%, whereas along the transverse direction the modal damping is 24%.
- When fluid dampers are added, the modal damping ratios of modes that involve large movements of the fluid dampers increase substantially (longitudinal, torsional, and transversal modes).

Time–History Response Analysis

The bridge response is computed by inducing, as support motions along the transverse and longitudinal directions, the recorded acceleration time histories at the free field and the amplified acceleration time histories at the crest of the embankment to the idealized model shown in Fig. 5. The fault normal component is applied along the transverse direction while the fault parallel component is applied simultaneously along the longitudinal direction. The time history response analysis is conducted on the bridge with elastomeric pads and nonlinear fluid dampers (Case 1), the bridge with elastomeric pads (Case 2), and the bridge with integral abutment (Case 3), subjected to the ground motions listed in Table 1. The macroscopic force–displacement laws of the various substructure elements of the bridge appearing in Table 1 of the companion paper have been presented and discussed in that paper. Our two-dimensional nonlinear response analysis under the

Table 3. Modal Frequencies, ω_j (rad/s) and Damping Ratios, ξ_j (%), of the 91/5 Overcrossing under Moderate Earthquake Loading

	Case 2 (abutment: $G=20$ MPa, $\eta=0.40$; center bent: $G=56$ MPa, $\eta=0.12$; nominal amplitude of fluid dampers $u_0=2$ in.)				
Bridge structure	Modes		Undamped ω_j (rad/s)	Damped ω_j (rad/s)	ξ_j (%)
Bridge with integral abutment	1	First vertical (antisymmetric)	8.7366	$8.7353+0.4624i$	5.29
	2	Second vertical (symmetric)	10.897	$10.904+0.6343i$	5.81
	3	First transverse	17.154	$17.548+2.1811i$	12.34
	4	Longitudinal	22.988	$20.801+14.963i$	58.39
	5	Torsional/vertical	23.526	$24.686+2.9479i$	11.86
	6	Third vertical (symmetric)	23.275	$23.492+2.4673i$	10.45
Bridge with pads only	1	Longitudinal	7.6837	$7.6803+0.4313i$	5.61
	2	Torsional	7.9938	$7.9989+0.4557i$	5.69
	3	First vertical (symmetric)	9.6029	$9.5987+0.5442i$	5.66
	4	First transverse	10.806	$10.836+0.6947i$	6.40
	5	Second vertical (symmetric)	10.940	$10.934+0.6324i$	5.77
	6	Second transverse	20.942	$21.108+2.6958i$	12.67
Bridge with pads and fluid dampers	1	Longitudinal	7.6837	$8.1866+2.4706i$	28.89
	2	Torsional	7.9938	$8.8755+13.983i$	84.43
	3	First vertical (symmetric)	9.6029	$8.7969+0.8466i$	9.78
	4	First transverse	10.806	$17.835+4.3610i$	23.75
	5	Second vertical (symmetric)	10.940	$10.926+0.6223i$	5.69
	6	Second transverse	20.942	$11.550+14.506i$	78.23

11 strong ground motions listed in Table 1 generated a wealth of time histories some of which are presented in the report by Makris and Zhang (2002).

The results of our analysis are presented in summary plots where peak response values are presented for all the 11 earthquake motions used in this study. Fig. 7 shows the peak total accelerations and relative displacements along the transverse and longitudinal directions near the east end of the deck (Point A). The same quantities normalized to the response of the configuration with integral abutments are shown in Fig. 8. The longitudinal response of the bridge is in accordance with what one expects intuitively. The bridge with sitting abutment is more flexible than that with integral abutments, so accelerations are smaller and displacements are larger. Damping reduces both displacements and

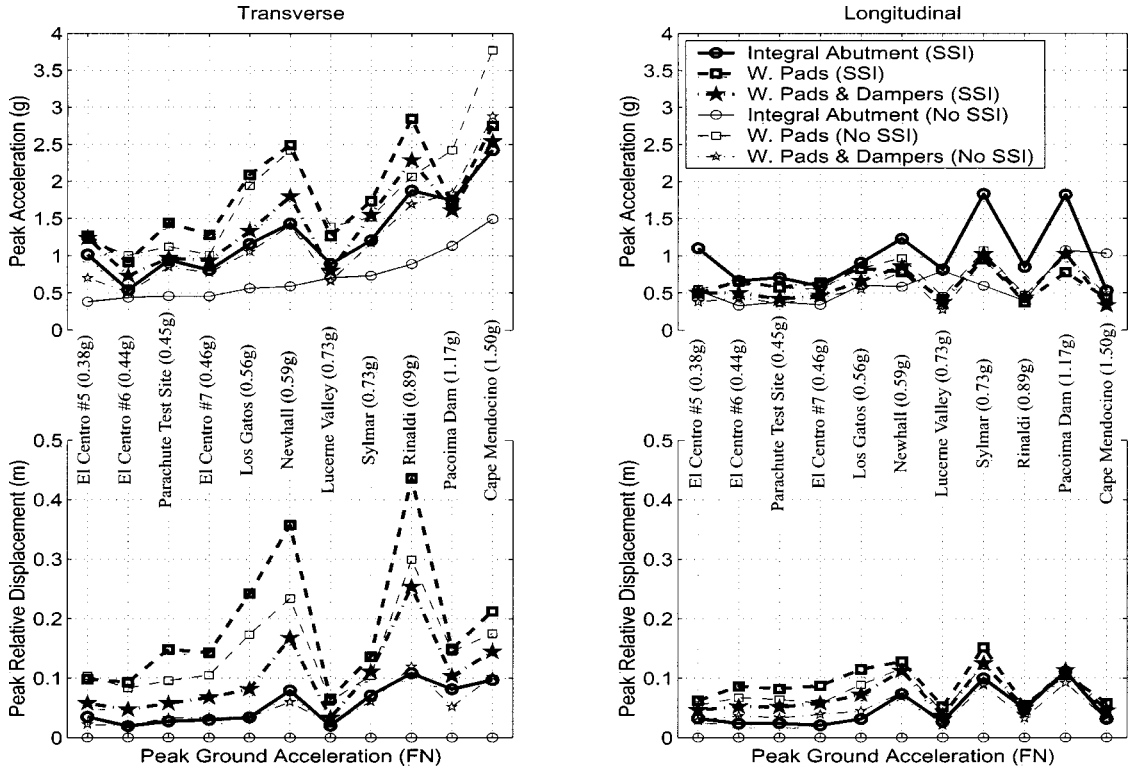

Fig. 7. Peak total accelerations (top) and peak relative displacements (bottom) near east end of deck (Point A) due to various earthquake motions ordered with increasing peak ground acceleration of the fault-normal component

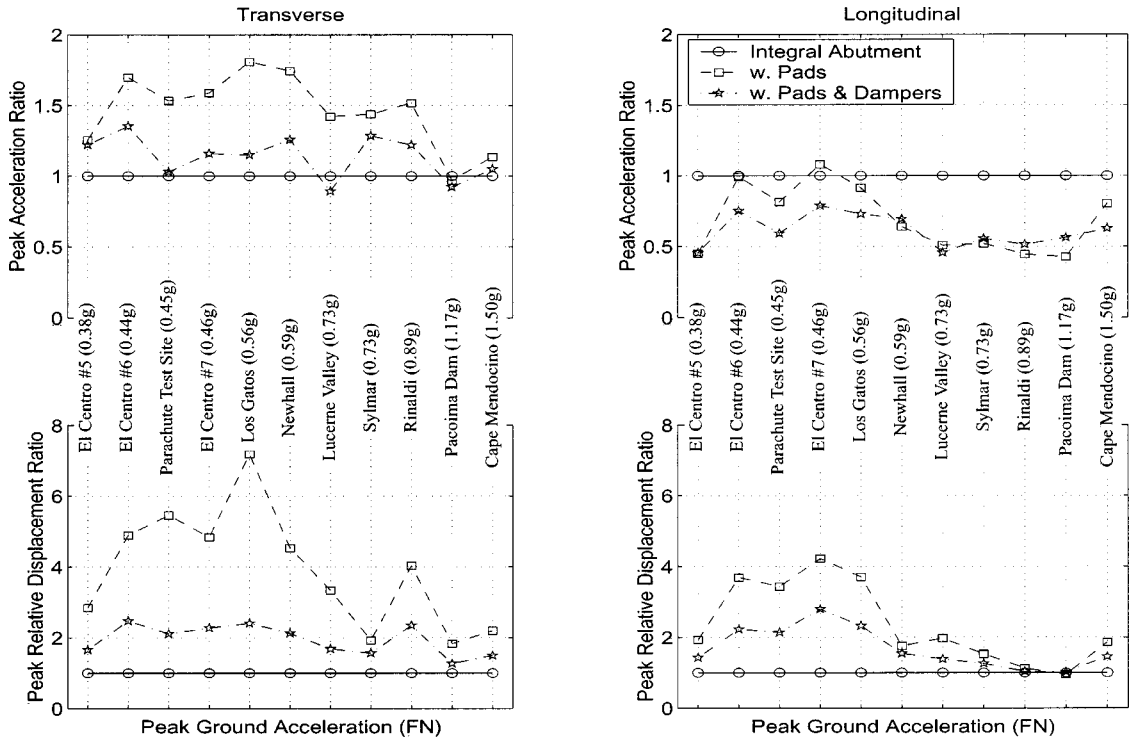

Fig. 8. Normalized bridge response quantities near east end of deck (point A) to the corresponding response quantities of bridge with integral abutments due to various earthquake motions ordered with increasing peak ground acceleration of the fault-normal component

accelerations of the flexible configuration. Figs. 7 and 8 (left-hand side) show that the transverse response of the bridge with integral abutments yields not only smaller relative displacements but also smaller accelerations. This can be explained by concentrating on the transverse modes of the two configurations that is the third mode (3rd) when integral abutments are considered and the fourth mode (4th) when sitting abutments are considered. In the case of integral abutments, the transverse mode is primarily a flexural mode, whereas in the case of sitting abutment the transverse mode is primarily a translational mode where the entire deck translates sideways without flexing appreciably. This results in larger displacements at the deck ends and also larger accelerations. Supplemental damping reduces both displacements and accelerations but the response of the bridge with sitting abutments appears to underperform the response of the bridge with integral abutments. Fig. 9 plots the normalized response of the bridge computed without soil–structure interaction to the response of the bridge computed with soil–structure interaction. For the configuration with pads and dampers (Case 1), this ratio is below unity, indicating that soil-structure interaction increases both accelerations and displacements.

Figs. 10–12 plot total accelerations and relative-to-the-ground displacements at the mid-span (Point B). The trend of accelerations and displacements along the longitudinal directions resembles the trend that one observes at Point A (east of the deck near the abutment). Along the transverse direction, the results for accelerations and displacements of the two configurations are mixed. This is because the midspan moves sideways approximately the same amount, regardless of whether the transverse movement is the result of a primarily flexural mode or of a primarily translational mode. Fig. 12 indicates that an analysis of the bridge response that neglects the effect of soil–structure interaction considerably underestimates the transverse and longitudinal displacements of the midspan.

The results of Figs. 7–12 indicate that the lengthening of the period of an overcrossing by introducing seat-type abutments reduces the longitudinal accelerations of the deck but increases the translational accelerations. The introduction of damping is beneficial; but the configuration with integral abutment is shown to yield the most favorable response. Soil–structure interaction is responsible for increasing displacements while having a mixed effect on accelerations.

Fig. 13 plots peak forces that develop at the deck ends due to various earthquake motions. Clearly, the configuration with integral abutments results in higher forces which, in some cases, are as high as one-half (1/2) of the deck weight. The configuration with pads alone results in the smaller forces which are approximately 5% of the deck weight. This result is expected since the 4 MN of the vertical reaction at each deck end is approximately 0.16 W and with a coefficient of friction, $\mu \approx 0.3$, the maximum horizontal force is $0.3 \times 0.16\ W \approx 0.05\ W$.

Fig. 14 plots the transverse and longitudinal forces behind the end abutments for the three configurations of interest and the two cases with and without soil–structure interaction. The normalized forces to the forces of the bridge with integral abutments when soil–structure interaction is considered are shown in Fig. 15. Clearly, the isolated configuration reduces the longitudinal forces but not the transverse forces. Interestingly, the presence of fluid dampers yields transverse forces that are higher than the forces when the bridge has integral abutments.

Fig. 16 shows the normalized forces behind the abutments computed without soil–structure interaction to the corresponding forces computed with soil–structure interaction. For all but the Cape Mendocino record, the forces without soil–structure interaction are smaller than the forces with soil–structure interaction. In some cases, such as the El Centro Array No. 5 record or the Newhall and Sylmar records, the force ratio is as low as 0.5,

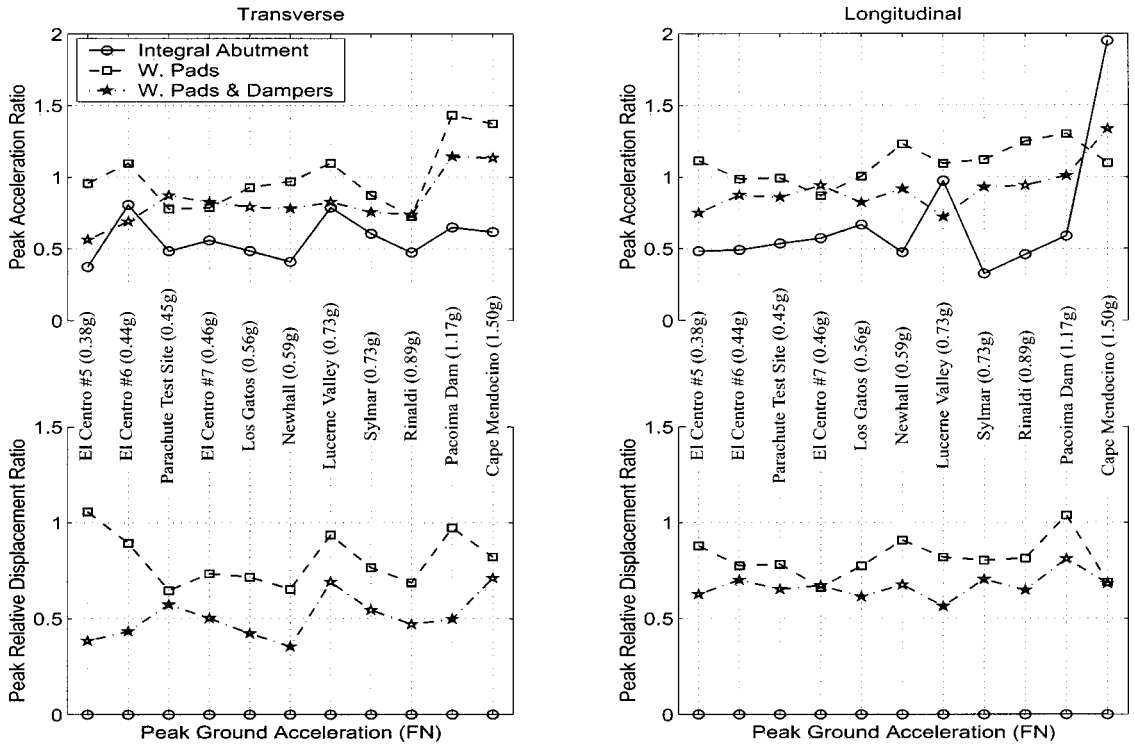

Fig. 9. Normalized bridge response quantities near east end of deck (point A) computed without soil–structure interaction to the corresponding response quantities computed with soil–structure interaction due to various earthquake motions ordered with increasing peak ground acceleration of the fault-normal component

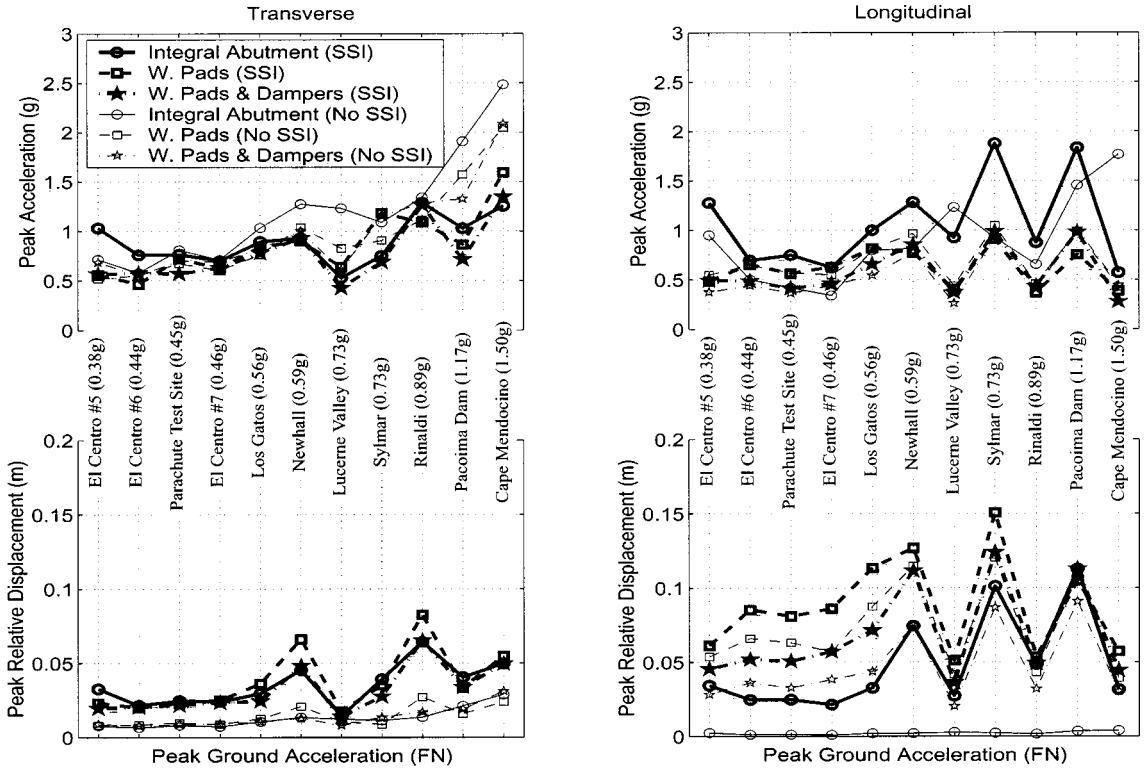

Fig. 10. Peak total accelerations (top) and peak relative displacements (bottom) at midspan (Point B) due to various earthquake motions ordered with increasing peak ground acceleration of the fault-normal component

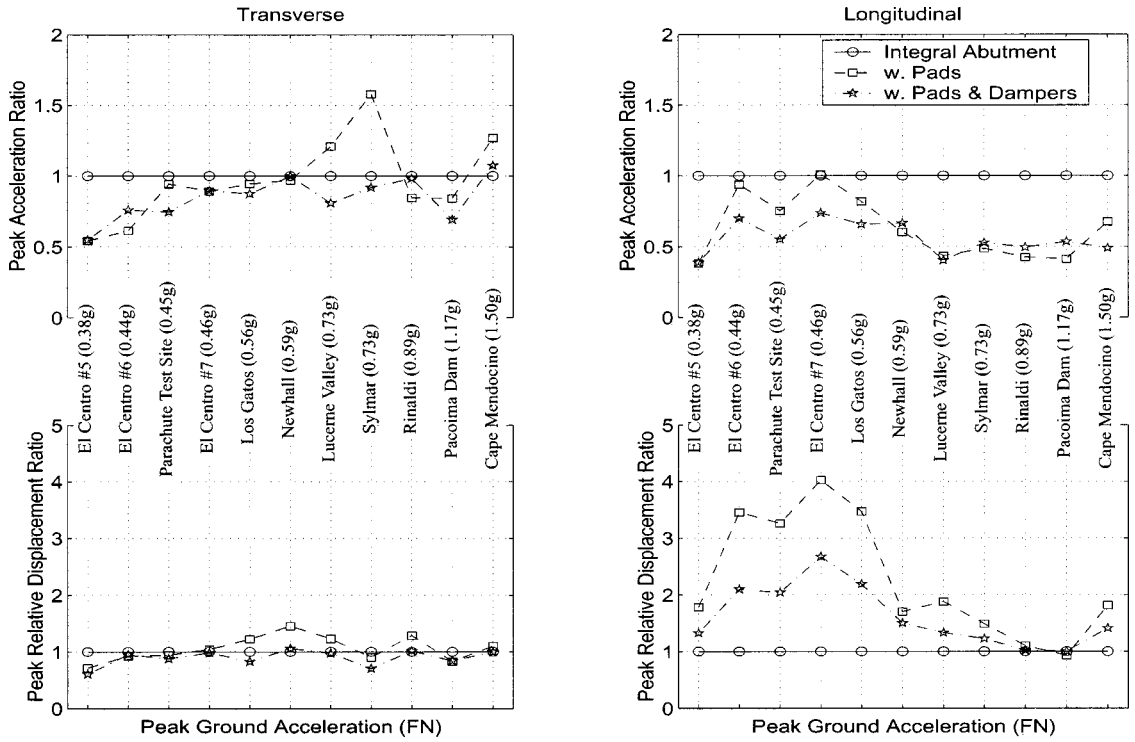

Fig. 11. Normalized bridge response quantities at midspan (Point B) to the corresponding response quantities of bridge with integral abutments due to various earthquake motions ordered with increasing peak ground acceleration of the fault-normal component

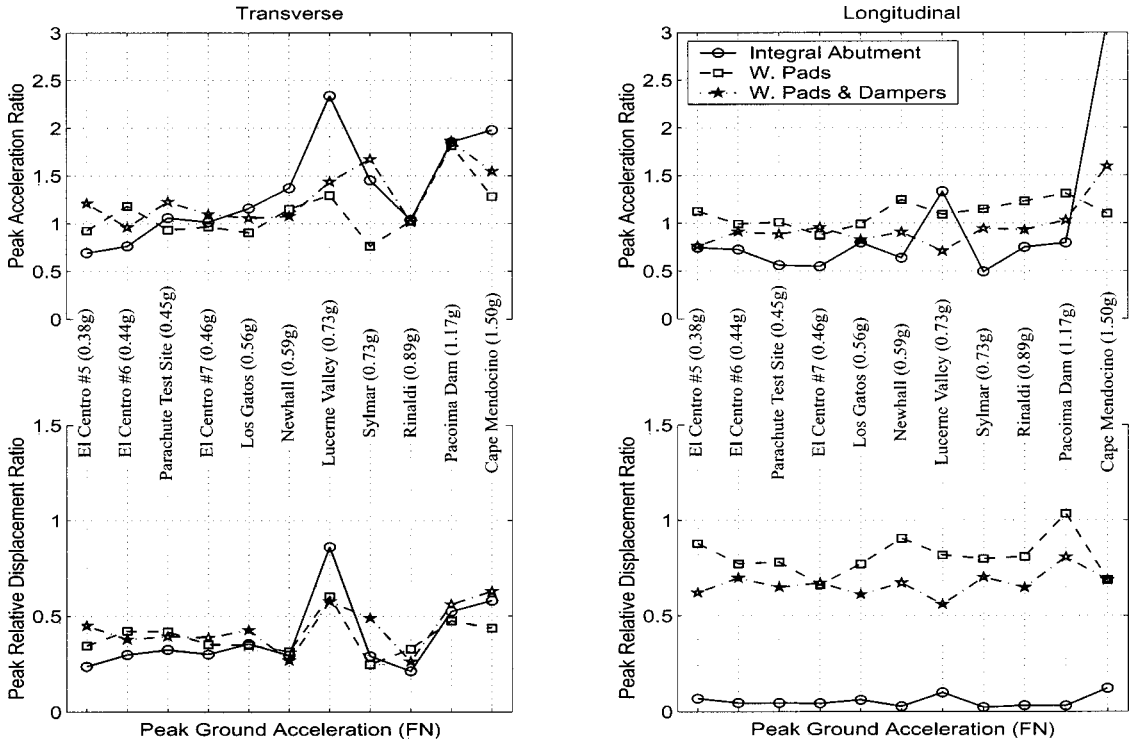

Fig. 12. Normalized bridge response quantities at midspan (Point B) computed without soil–structure interaction to the corresponding response quantities computed with soil–structure interaction due to various earthquake motions ordered with increasing peak ground acceleration of the fault-normal component

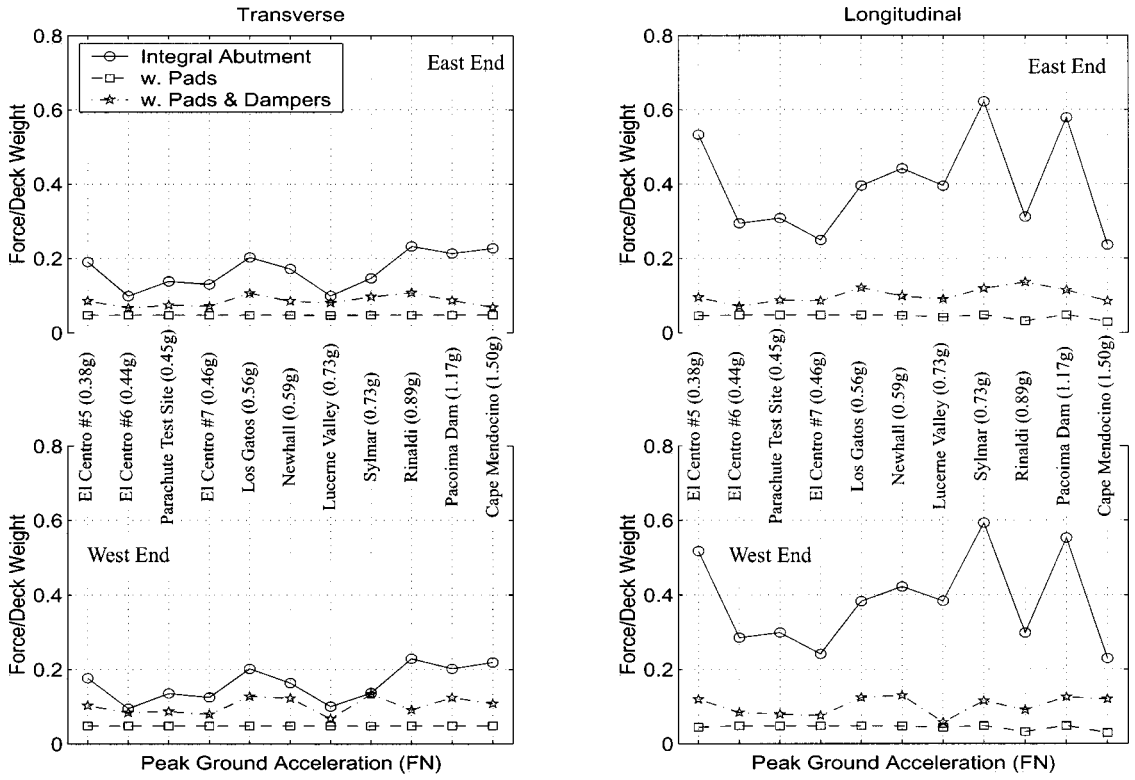

Fig. 13. Peak forces at deck ends due to various earthquake motions ordered with increasing peak ground acceleration of the fault-normal component

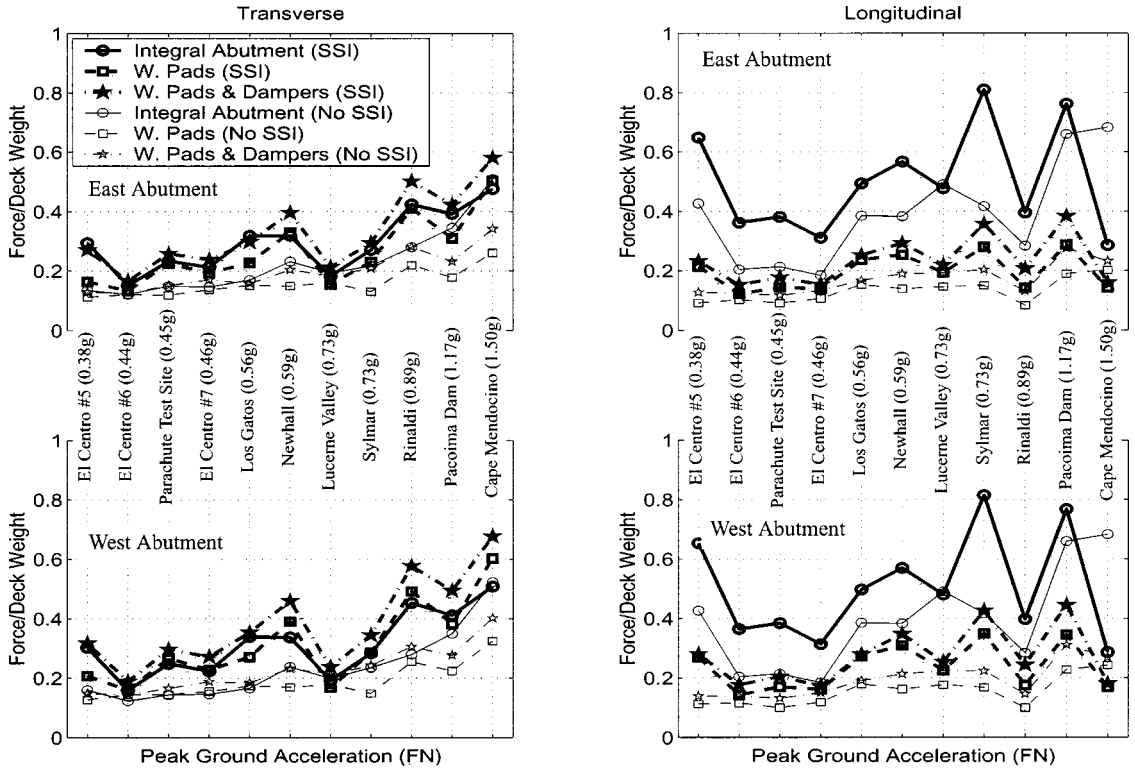

Fig. 14. Peak forces behind end abutments due to various earthquake motions ordered with increasing peak ground acceleration of the fault-normal component

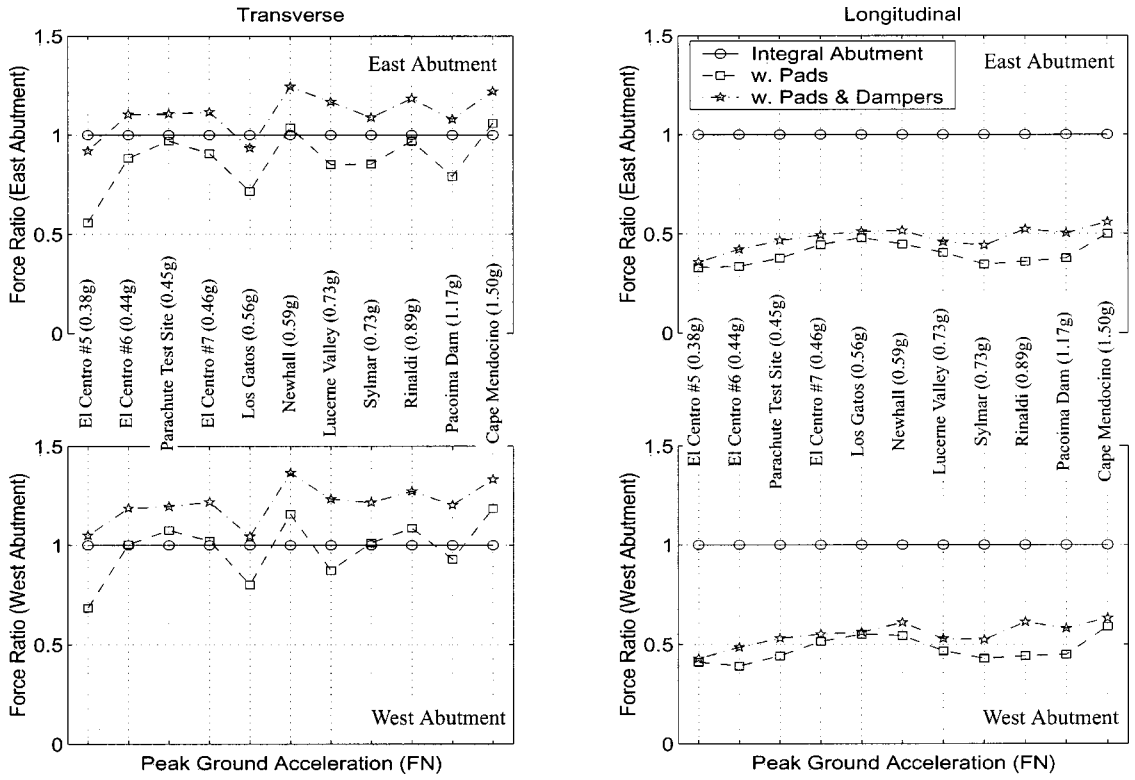

Fig. 15. Normalized forces behind end abutments to the corresponding forces of bridge with integral abutments due to various earthquake motions ordered with increasing peak ground acceleration of the fault-normal component

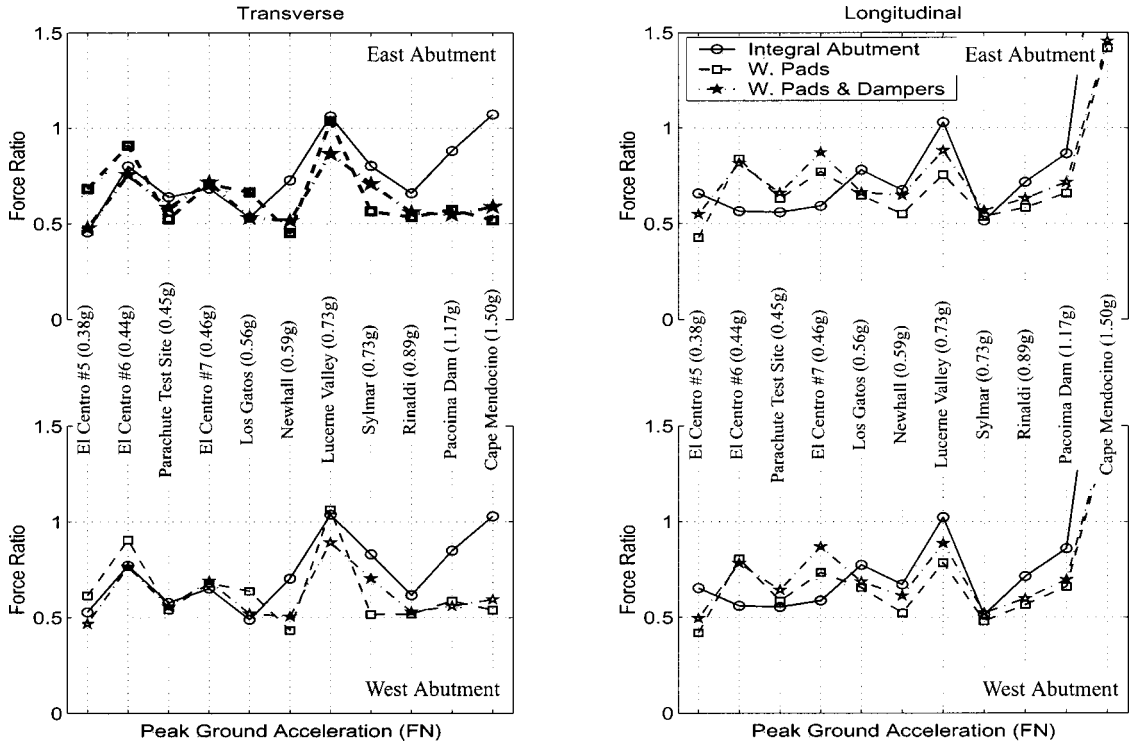

Fig. 16. Normalized forces behind end abutments computed without soil–structure interaction to the corresponding forces computed with soil–structure interaction due to various earthquake motions ordered with increasing peak ground acceleration of the fault-normal component

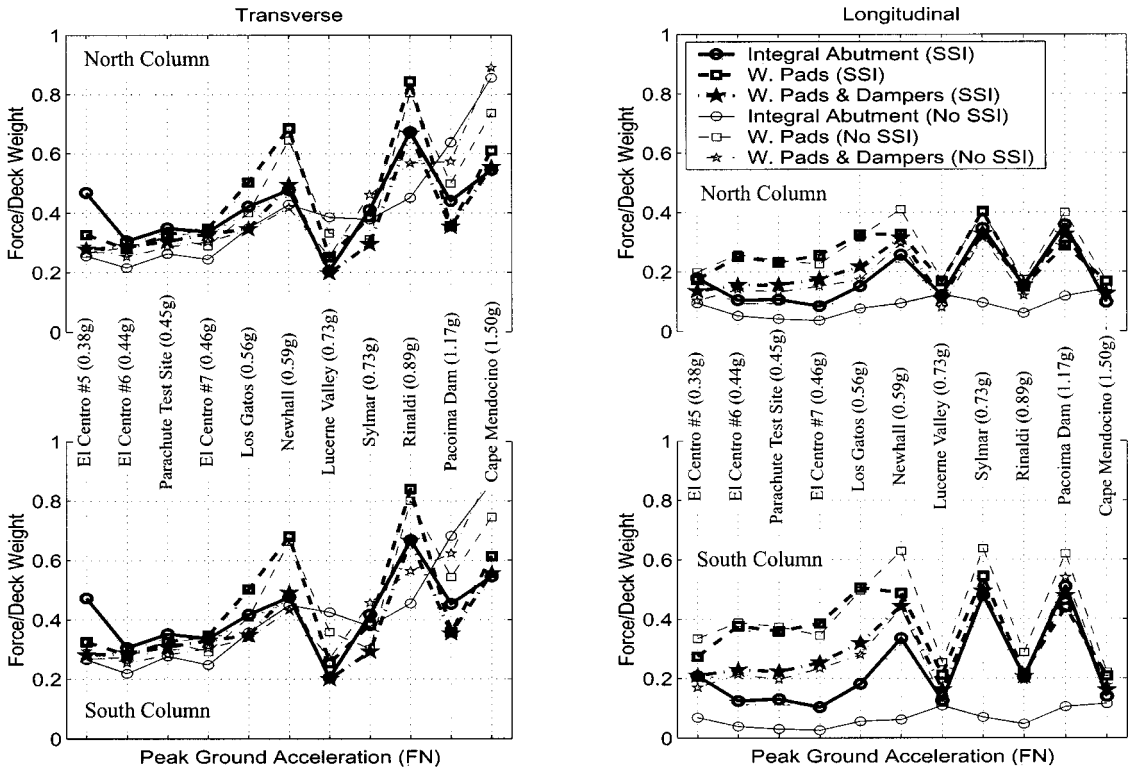

Fig. 17. Peak forces at base of center columns due to various earthquake motions ordered with increasing peak ground acceleration of the fault-normal component

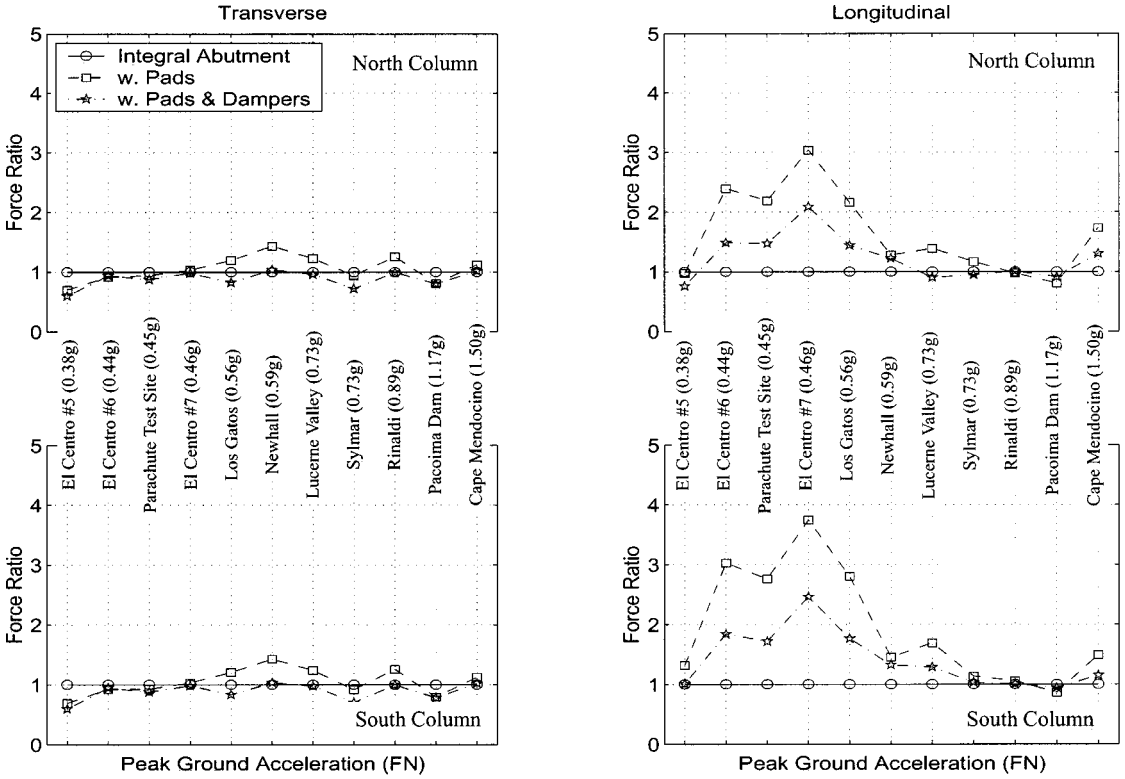

Fig. 18. Normalized forces at base of center columns to the corresponding forces of bridge with integral abutments due to various earthquake motions ordered with increasing peak ground acceleration of the fault-normal component

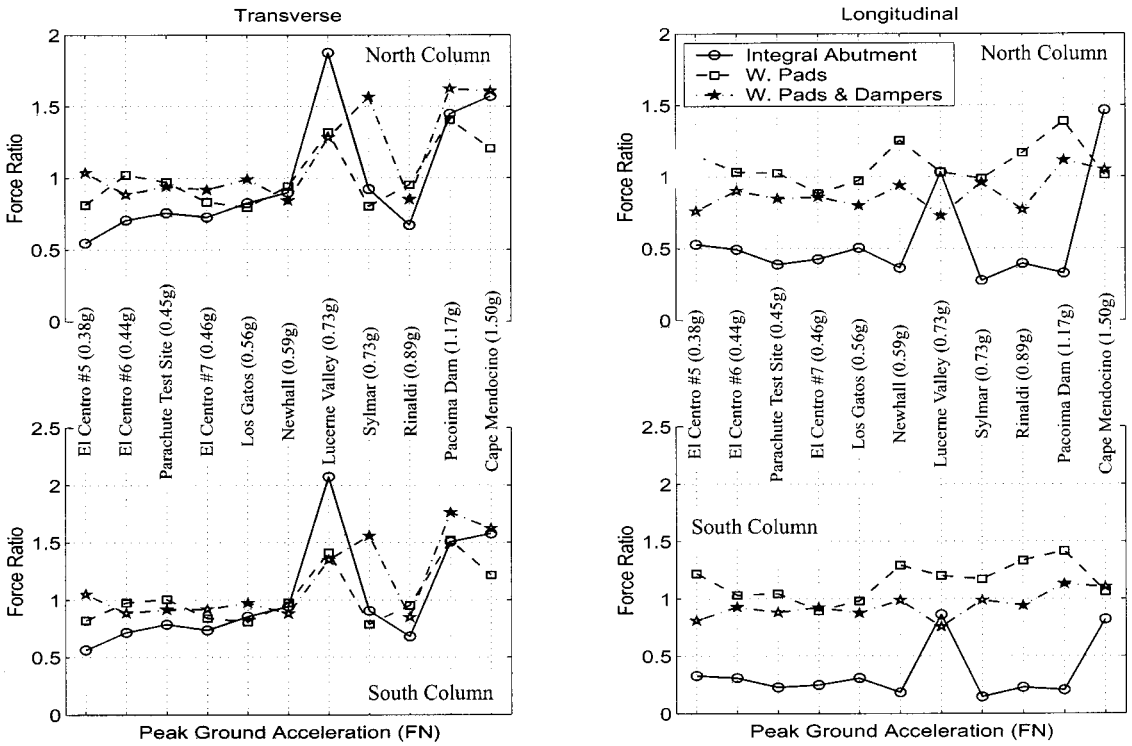

Fig. 19. Normalized forces at base of center columns computed without soil–structure interaction to the corresponding forces computed with soil–structure interaction due to various earthquake motions ordered with increasing peak ground acceleration of the fault-normal component

indicating that an analysis that neglects soil–structure interaction underestimates the forces appreciably.

Fig. 17 plots the transverse and longitudinal shear forces at the base of columns of the center bent for the three configurations of interest and the two cases with and without soil–structure interaction. The normalized forces to the corresponding forces of bridge with integral abutments when soil–structure interaction is considered are shown in Fig. 18. Along the transverse direction, the isolated bridge transmits approximately the same forces to the column bases as the bridge with integral abutment. Along the longitudinal direction, the differences are dramatic since, in some earthquakes, the column forces of the isolated bridge are more than two times the column forces of the bridge with integral abutments. Nevertheless, our analysis indicated that even when the bridge is isolated, the center columns remain practically elastic. Fig. 19 shows the normalized column forces computed without soil–structure interaction to the corresponding forces computed with soil–structure interaction. Other than the Lucerne Valley and Cape Mendocino records, the base shears of the center columns of the bridge with integral abutments are significantly underestimated when soil–structure interaction is neglected. When the bridge is isolated at the deck ends, the value of the base shears of the columns is relatively insensitive to the effect of soil–structure interaction.

Conclusions

This paper presents a case study on the seismic response of the 91/5 Overcrossing that is equipped with elastomeric bearings and fluid dampers at its end abutments. The analysis was conducted using the substructure method and a reduced-order stick model that were established elsewhere. The macroscopic constitutive laws of the main substructure elements of the 91/5 Overcrossing have been presented in the companion paper. Our two-dimensional nonlinear dynamic analysis revealed distinguishable trends that lead to the following conclusions:

- The first transverse mode of a bridge with integral abutments is a flexural mode, whereas, the first transverse mode of a bridge that is isolated at its end abutments is essentially a translational mode.
- The increased mobility of the deck ends due to the elastomeric bearings results in high acceleration which can be suppressed with supplemental damping. The response at the end abutments of an isolated bridge appears to underperform the response of the same bridge with integral abutments.
- When soil–structure interaction is neglected, the response of the isolated bridge is underestimated.
- The longitudinal forces at the backwall are reduced by one-half when the bridge is isolated at the end abutments. Isolation does not appear to have an effect in reducing backwall forces along the transverse direction. In contrast, the addition of fluid dampers in the isolation system yield transverse forces that exceed the forces transmitted when the bridge has integral abutments.
- When soil–structure interaction is neglected, both transverse and longitudinal forces at the backwall are underestimated. Under some earthquakes, the forces at the backwall calculated by including the effects of soil–structure interaction can be more than two times larger; in particular for the bridge with pads and dampers.
- When the bridge is isolated at the end abutments, the base shear at the center columns is larger than the corresponding forces of the bridge with integral abutment. This two to three times increase occurs primarily along the longitudinal direc-

tion. Despite this considerable increase, the center columns of the 91/5 Overcrossing remained nearly elastic even under the strongest shaking studied in this paper.
- When soil-structure interaction is neglected, the base shears of the center columns are, in general, significantly underestimated.

In summary, the reduced-order stick model, in association with concentrated springs and dashpots that realistically represent the behavior of the main substructure elements, can generate valuable results on the response of short bridges.

Acknowledgment

Partial financial support for this study was provided by the National Science Foundation under Grant No. CMS-9696241.

References

ABAQUS. (1997). *User's manual V5.7*, Hibbitt, Karlsson & Sorensen, Inc.

American Association of State Highway and Transportation Officials (AASHTO). (1999). *Guide specifications for seismic isolation design*, American Association of State Highway and Transportation Officials, Washington, D.C.

Applied Technical Council. (1993). *Seminar on Seismic Isolation, Passive Energy Dissipation, and Active Control, Rep. No. ATC-17-1*, Applied Technology Council, Redwood City, Calif.

Applied Technical Council. (2002). *Seminar on response modification technologies for performance-based seismic design, Rep. No. ATC-17-2*, Applied Technology Council, Los Angeles.

Chang, S. P., Makris, N., Whittaker, A. S., and Thompson, A. C. T. (2002). ''Experimental and analytical studies on the performance of hybrid isolation system.'' *Earthquake Eng. Struct. Dyn.*, 31(2), 421–443.

Dendrou, B., Werner, S. D., and Toridis, T. (1985). ''Three-dimensional response of a concrete bridge system to traveling seismic waves.'' *Comput. Struct.*, 20, 593–603.

Douglas, B. M., and Reid, W. H. (1982). ''Dynamic tests and system identification of bridges.'' *J. Struct. Div. ASCE*, 108(10), 2295–2312.

Federal Highway Administration (FHWA). (1995). ''Seismic retrofitting manual for highway bridges.'' *Publication No. FHWA-RD-94-052*, FHWA, McLeon, Va.

Imai, T., and Tonouchi, K. (1982). ''Correlations among seismic motion, ground conditions, and damage: Data on the Miyagiken-oki earthquake of 1978.'' *Proc., 3rd Int. Earthquake Miscorzonation Conf.*, Univ. of Washington, Seattle, Vol. 2, pp. 649–660.

Kramer, S. L. (1996). *Geotechnical earthquake engineering*, Prentice–Hall, Upper Saddle River, N.J.

Makris, N., and Chang, S. P. (1998). ''Effect of damping mechanisms on the response of seismic isolated structures.'' *Rep. No. PEER-98/06*, Univ. of California, Berkeley, Calif.

Makris, N., and Chang, S. P. (2000a). ''Response of damped oscillators to cycloidal pulses.'' *J. Eng. Mech.*, 126(2), 123–131.

Makris, N., and Chang, S. P. (2000b). ''Effect of viscous, viscoplastic and friction damping on the response of seismic isolated structures.'' *Earthquake Eng. Struct. Dyn.*, 29(1), 86–107.

Makris, N., Badoni, D., Delis, E., and Gazetas, G. (1994). ''Prediction of observed bridge response with soil–pile–structure interaction.'' *J. Struct. Eng.*, 120(10), 2992–3011.

Maragakis, E. A., and Jennings, P. C. (1987). ''Analytical models for the rigid body motions of skew bridges.'' *Earthquake Eng. Struct. Dyn.*, 15(8), 923–944.

McCallen, D. B., and Romstad, K. M. (1994). ''Analysis of a skewed short-span, box-girder overpass.'' *Earthquake Spectra*, 10(4), 729–755.

Papanikolas, P. K. (2002). ''Deck superstructure and cable stays of the Rion-Antirion bridge.'' *Proc., 4th Nat. Conf. on Steel Structures*, Patros, Greece.

Seed, H. B., Wong, R. T., Idriss, I. M., and Tokimatsu, K. (1986). ''Moduli and damping factors for dynamic analyses of cohesionless soils.'' *J. Geotech. Eng.*, 112(11), 1016–1032.

Skinner, R. I., Robinson, W. H., and McVerry, G. H. (1993). *An introduction to seismic isolation*, Wiley, Chichester, U.K.

Symth, A. W., Masri, A. F., Abdel-Ghaffar, A. M., and Nigbor, R. N. (2000). ''Development of a nonlinear multi-input.multi-output model for the Vincent Thomas Bridge under earthquake excitations.'' *Proc., 12th World Conf. on Earthquake Engineering*, Paper No. 2211, Upper Hutt, New Zealand.

Zhang, J., and Makris, N. (2001). ''Seismic response analysis of highway overcrossings including soil–structure interaction.'' *Rep. No. PEER-01/02*, Univ. of California, Berkeley, Calif.

Zhang, J., and Makris, N. (2002a). ''Kinematic response functions and dynamic stiffnesses of bridge embankments.'' *Earthquake Eng. Struct. Dyn.*, 31, 1933–1966.

Zhang, J., and Makris, N. (2002b). ''Seismic response analysis of highway overcrossing including soil–structure interaction.'' *Earthquake Eng. Struct. Dyn.*, 31, 1967–1991.

Makris, N., and Zhang J. (2002).

Zhang, J., Makris, N., and Delis, T. (2004). ''Structural characterization of modern highway overcrossings—Case study.'' *J. Struct. Eng.*, 130(6), 846–860.